3032
doi:10.1017/S1431927622011333
Microsc. Microanal. 28 (Suppl 1), 2022

Automation of Supported Nanoparticle Recognition in Low Contrast STEM Images

Mads Lützen[1], Daniel Kelly[1], Thomas E. L. Smitshuysen[2] and Christian D. Damsgaard[1,2*]

[1.] Technical University of Denmark - Nanolab, Kgs. Lyngby, Hovedstaden, Denmark.
[2.] Technical University of Denmark - Physics, Kgs. Lyngby, Hovedstaden, Denmark.
[*] Corresponding author: cdda@dtu.dk

Automating the recognition and measurement of nanoparticles would allow for computation of large datasets that would otherwise be impractical to compute manually. In addition to the time costs, lack of contrast in specimens can also make distinguishing particle geometries imprecise, especially in multiphase or supported materials. An example would be investigating sintering behavior in industrial catalysts, where small nanoparticles of varying size are distributed on large supports [1]. Presented here are considerations of an algorithm to address these issues.

Although high angular annular dark field (HAADF) scanning transmission electron microscopy (STEM) results in Z-contrast, ultimately mass-thickness effects will also contribute to the relative contrast within images. In images with multiple species, such as supported nanoparticles (figure 1), we must consider measurable contrast of a singular object (nanoparticle) as the relative difference in intensity between the closest contour outside the object and the contour of the object. A binary image would, by this definition, have the maximum contrast. Here it is simple to find the contour of an object. A high contrast image is here described by having two or more groups of distinct intensity values that can be separated by the use of an automated thresholding method, a well-known example being the Otsu algorithm [2]. However, in low contrast images, neither manual thresholding nor using the multi-Otsu algorithm are capable of finding the true contours, as shown in figure 1a, 1b. The sample investigated here consists of CoCuGa alloy nanoparticles with different sizes and composition on SiO_2 support. This makes it a difficult system to analyze, especially with a fully automatic algorithm.

The method presented here occurs as follows: the set of all contours in an image is found by applying a threshold at all pixel values and determining the contours for each threshold. Within this set, the true contours corresponding to the morphology of the target nanoparticles are present, however they co-exist alongside contours from the support, background and noise. To separate the nanoparticles from the rest of the contours, a set of constraints is defined that are independent from the characteristics that are to be determined, e.g. area, perimeter, circularity. With the appropriate choice of constraints, the nanoparticles can be identified automatically and precisely, in good agreement with manual methods. Our constraints sort the contours based on their convexity, mean normal-gradient and the relative area difference between them. All of these criteria are automatically determined based on the full set of contours. Application of the algorithm developed here on the same dataset as in figure 1a, 1b yields well-defined and recognizable nanoparticle contours shown in figure 1c. Comparing our algorithm to the two other methods shows a narrower distribution of contours with fewer outliers both towards smaller and larger contours, this can be seen in figure 1d. Our algorithm differs from the other methods by incorporating multiple morphological descriptors for the particles that can be tailored based on pre-existing knowledge of the specimen, compared to the other methods that operate based on either single-value (manual and Otsu) or multiple (multi-Otsu) thresholds.

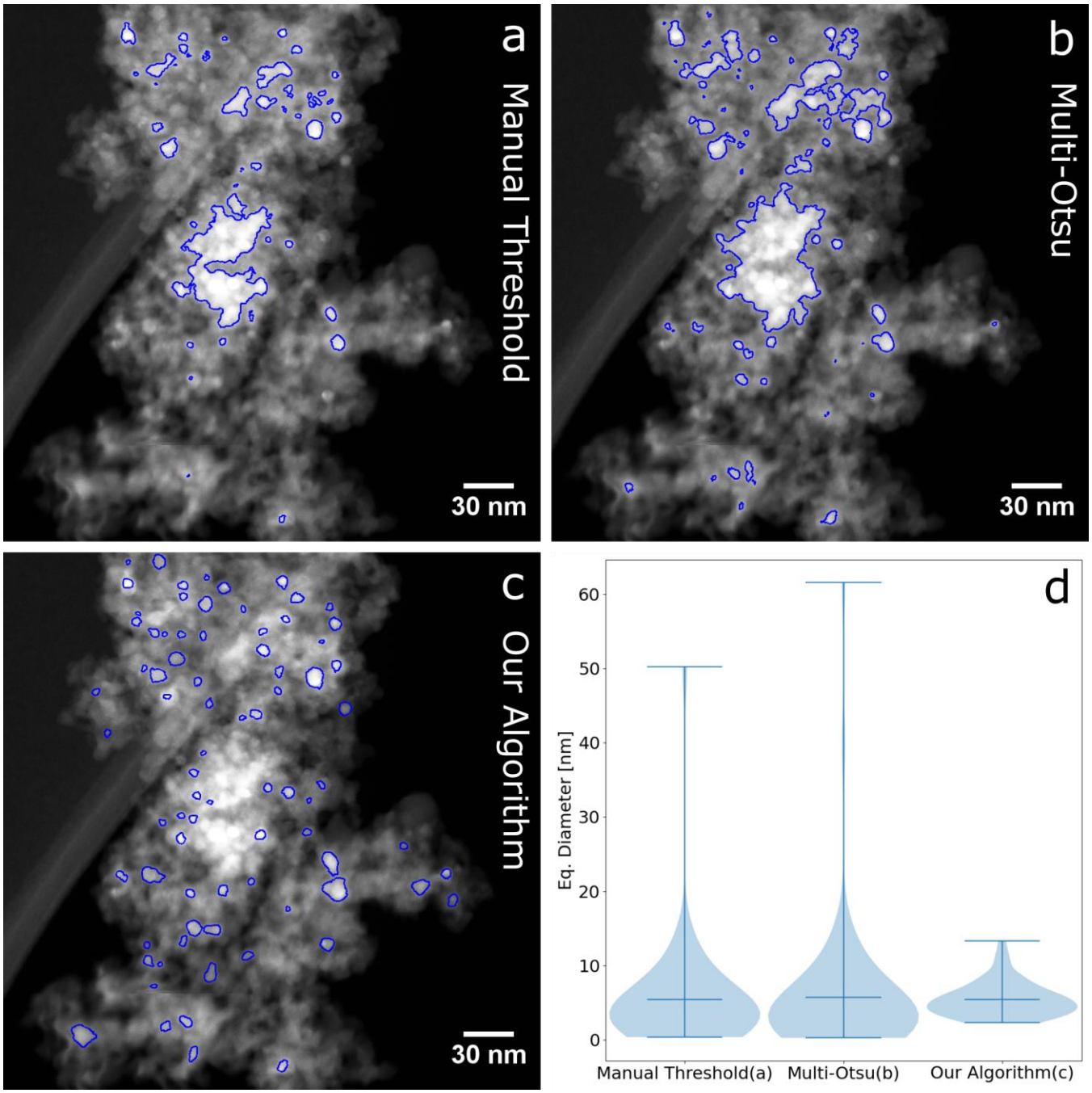

Figure 1. HAADF-STEM image of CoCuGa alloy nanoparticles supported on SiO_2. Indicated with blue the contours found with a manual threshold (threshold >= 187 of 255) (a) the multi-Otsu threshold (threshold >= 164 of 255) (b) and with our algorithm (c). In (d) violinplot of the eq. diameter distributions.

https://doi.org/10.1017/S1431927622011333 Published online by Cambridge University Press

References:

[1] K. Dembélé et al., ChemCatChem **13** (2021), p. 1920-1930. doi: 10.1002/cctc.202001074

[2] N. Otsu, IEEE Transactions on Systems, Man and Cybernetics **9** (1979), p. 62-66. doi: 10.1109/TSMC.1979.4310076

https://doi.org/10.1017/S1431927622011333 Published online by Cambridge University Press